

(11) **EP 2 952 466 A1**

(12)

EUROPEAN PATENT APPLICATION

(43) Date of publication:

09.12.2015 Bulletin 2015/50

(51) Int Cl.:

B66C 13/06 (2006.01) B66C 13/46 (2006.01) B66C 13/08 (2006.01)

(21) Application number: 15169336.3

(22) Date of filing: 27.05.2015

(84) Designated Contracting States:

AL AT BE BG CH CY CZ DE DK EE ES FI FR GB GR HR HU IE IS IT LI LT LU LV MC MK MT NL NO PL PT RO RS SE SI SK SM TR

Designated Extension States:

BA ME

Designated Validation States:

MA

(30) Priority: 02.06.2014 DE 102014008094

(71) Applicant: Liebherr-Werk Nenzing GmbH

6710 Nenzing (AT)

(72) Inventors:

 Schneider, Dr.-Ing. Klaus 88145 Hergatz (DE)

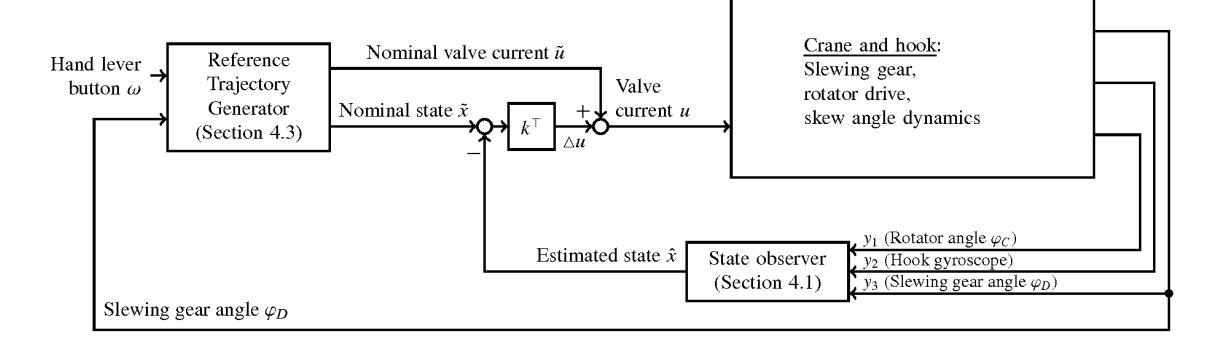
- Sawodny, Prof. Dr.-Ing. Oliver 70186 Stuttgart (DE)
- Schaper, DI UIf 70569 Stuttgart (DE)
- Arnold, Dr.-Ing. Eckhard 98693 Ilmenau (DE)
- (74) Representative: Laufhütte, Dieter Lorenz Seidler Gossel Rechtsanwälte Patentanwälte Partnerschaft mbB Widenmayerstrasse 23 80538 München (DE)

(54) METHOD FOR CONTROLLING THE ORIENTATION OF A CRANE LOAD AND A BOOM CRANE

(57) This invention relates to a method for controlling the orientation of a crane load, wherein a manipulator for manipulating the load is connected by a rotator unit to a hook suspended on ropes and the skew angle η_L of the load is controlled by a control unit of the crane, charac-

terized in that the control unit is an adaptive control unit wherein an estimated system state of the crane system is determined by use of a nonlinear model describing the skew dynamics during operation.

Fig. 9



EP 2 952 466 A1

Description

10

15

20

30

35

40

45

50

[0001] The invention relates to a method for controlling the orientation of a crane load, wherein a manipulator for manipulating the load is connected by a rotator unit to a hook suspended on ropes and the skew angle of the load is controlled by a control unit of the crane.

[0002] In small and midsize harbours, boom cranes are used for multiple applications. These include bulk cargo handling and container transloading. An example for a boom crane used in small and midsize harbours with mixed freight types is depicted in Figure 1. Currently, the level of process automation is comparatively low and container transloading is done manually by crane operators. However, the general trend of logistic automation in harbours requires higher container handling rates, which can be achieved by increasing the level of process automation.

[0003] On boom cranes, containers are mounted to the crane hook using spreaders (manipulators), see Figure 2. Spreaders can only be locked to containers after they have been precisely landed on them. This means that the position and the orientation of the spreader have to be adapted to the container for successfully grabbing the container with the spreader. The spreader orientation, which is also defined as the skew angle, is controlled using a hook-mounted rotator motor.

[0004] Since wind, impact, and uneven load distribution can cause skew vibrations, an active skew control is desirable for facilitating crane operation, improving positioning accuracy, and increasing turnover. Positioning the spreader requires damping the pendulum oscillations, which can be done either manually by the operator or automatically using anti-sway systems. Adapting the spreader orientation requires damping the torsional oscillations ("rotational vibrations" or "skewing vibrations") using a rotational actuator, which is regularly done manually.

[0005] A few technical solutions for a skew control are known from the state of the art and which are mostly designed for a gantry crane. Due to specific properties of such cranes these implementations of skew controls are mostly not compliant with differing crane designs. In particular boom cranes comprise a longer rope length and a much smaller rope distance which yields to lower torsional stiffness compared to gantry cranes. This increases the relevance of constraints and also results in lower eigenfrequencies. Second, arbitrary skew angles are possible on boom cranes, while gantry cranes can only reach skew angles of a few degrees. Third, the well-established visual load tracking mechanism of gantry cranes using cameras and markers cannot be applied to boom cranes.

[0006] For instance, a solution for a skew control system is known from EP 1 334 945 A2 performing optical position measurements (e.g. camera based) for detecting the skew angle. However, such system may become unavailable during night or during bad weather conditions.

[0007] Another method for controlling the orientation of the crane load is known from DE 100 29 579 and DE 10 2006 033 277 A1. There, the hook suspended on ropes has a rotator unit containing a hydraulic drive, such that the manipulator for grabbing containers can be rotated around a vertical axis. Thereby, it is possible to vary the orientation of the crane loads. If the crane operator or the automatic control gives a signal to rotate the manipulator and thereby the load around the vertical axis, the hydraulic motors of the rotator unit are activated and a resulting flow rate causes a torque. As the hook is suspended on ropes, the torque would result in a torsional oscillation of the manipulator and the load. To position the load at a specific angle, this torsional oscillation has to be compensated. However, the solutions known from DE 100 29 579 and DE 10 2006 033 277 A1 use linear models for describing the skew motion. Such linear models are only valid in a small neighborhood around the steady state, i.e. only small deflection angles can be used. Further, the systems known from DE 100 29 579 and DE 10 2006 033 277 A1 employ a state observer which needs the second derivative of a position measurement. Such a double differentiation is disadvantageous due to noise amplification. Furthermore, both systems known from DE 100 29 579 and DE 10 2006 033 277 A1 require knowledge of the load inertia which varies heavily with the load mass. Especially in DE 10 2006 033 277 A1, a time-consuming calculation method is used for estimating the load inertia.

[0008] It is the objection of the invention to provide an improved method for controlling the skew angle of a crane, in particular of a boom crane.

[0009] The aforementioned object is solved by a method according to the feature combination of claim 1. Preferred embodiments are subject matter of dependent claims 2 to 13.

[0010] According to the features of claim 1 the method is performed on a control unit of a crane comprising a manipulator for manipulating the orientation of a load connected by a rotator unit to a hook suspended on ropes. For improvement of the operating of the crane the skew angle of the load is controlled by a control unit of the crane.

[0011] In the following a rotation of the manipulator (spreader) and/or crane load (e.g. container) around the vertical axis is described as skew motion. The heading or yaw of a load is called skew angle and rotation oscillations of the skew angle are called skew dynamics.

⁵⁵ **[0012]** The expression hook defines the entire load handling devic excluding the spreader.

[0013] A control of the skew angle normally requires a feedback signal which is usually based on a measurement of the current system status. However, implementation of a skew control according to the invention requires states of the boom crane which cannot be measured or which are too disturbed to be used as feedback signals.

[0014] Therefore, the present invention recommends that one or more required states are estimated on the basis of a model describing the skewing dynamics during the crane operation. Further, a nonlinear model is used for describing the skew dynamics of the crane during operation instead of a linear model as currently applied by known skew controls. Implementation of a non-linear model enables consideration of the non-linear behaviour of the skew dynamics over a wider range or the full range of the possible skewing angle of the load. Since boom cranes permit a significantly larger skewing angle than gantry cranes the present invention essentially improves the performance and stability of the skew control applied to boom cranes.

[0015] According to the present invention a non-linear model is used which allows using larger deflection angles (up to 90°). Larger deflection angles yield larger reactive torques and therefore faster motion.

[0016] Further, the present invention does not require any optical sensors to improve the system availability and system reliability. No optical position measurement has to be performed for detecting the skew angle as known from the state of the art.

10

20

30

35

40

45

50

55

[0017] In the method for controlling the orientation of a crane load of the present invention, torsional oscillations are avoided by an anti-torsional oscillation unit using the data calculated by the dynamic non-linear model. This anti-torsional oscillation unit uses the data calculated by the dynamic non-linear model to control the rotator unit such that oscillations of the load are avoided. The anti-torsional oscillation unit can generate control signals that counteract possible oscillations of the load predicted by the dynamical model. The rotator unit includes an electric and/or hydraulic drive. The anti-torsional oscillation unit can generate signals for activating the rotator motor, thereby applying torque generated by a hydraulic flow rate or electric current.

[0018] In particular, the non-linearity included in the model describing the skew dynamics refers to the non-linear behaviour of the resulting reactive torque caused by torsion of the load, i.e. the ropes. For instance, the reactive torque increases until a certain skew angle of the load is reached, for instance of about 90 degrees. By excessing said certain skew angle the reactive torque decreases due to twisting of the ropes. The skew dynamic model preferably includes one or more non-linear terms or expressions representing the non-linear behaviour as described before.

[0019] Former controller architectures as described before require the mass of the load and most importantly, the moment of inertia of the load as an input parameter. However, the distribution of mass inside the load, e.g. a container, is unknown and therefore the moment of inertia of the load is not known, either. Therefore, known prior art control architectures estimate the moment of inertia of the load on the basis of a complex and computationally intensive process. According to a preferable aspect of the present invention the implemented non-linear model for estimation of the system state is independent on the load mass and/or the moment of inertia of the load mass. Consequently, the performance of the skew control significantly increases while reducing the processor load and usage of the control unit.

[0020] In particular, the method according to a further preferable aspect does not require a Kalman filter for estimation of the system state.

[0021] In a preferred embodiment of the present invention the estimated system state includes the estimated skew angle and/or the velocity of the skew angle and/or one or more parasitic oscillations of the skew system. A possible parasitic oscillation which influences the skew dynamics may be caused by the slackness of the hook, for instance. Further, system state may further include besides the estimates parameters several parameters which are directly or indirectly measured by measurement means of the crane.

[0022] The control unit is preferable based on a two-degree of freedom control (2-DOF) comprising a state observer for estimation of the system state, a reference trajectory generator for generation of a reference trajectory in response to a user input and a feedback control law for stabilization of the nonlinear skew dynamic model.

[0023] This means that a control signal for controlling the rotator drive of the rotator unit and/or a slewing gear and/or any other drive of the crane comprises a feedforward signal from the reference trajectory generator and a feedback signal to stabilize the system and reject disturbances. The feedforward control signal is generated by the reference trajectory generator and designed in such a way that it drives the system along a reference trajectory under nominal conditions (nominal input trajectory). Deviation from a nominal state (nominal state trajectory) defined by the reference trajectory generator are determined by using the estimated state determined by the state observer on the basis of the non-linear model for skew dynamics. Any deviation is compensated by a feedback signal determined from the nominal and estimated state using a feedback gain vector. The resulting compensated signal is used as the feedback signal for generation of the control signal.

[0024] For estimation of the system state considering the skew dynamics the state observer preferably receives measurement data comprising at least the drive position of the rotator unit and/or the inertial skewing rate and/or the slewing angle of the crane. These parameters may be measured by certain means installed at the crane structure. For instance, the drive position of the rotator may be measured by an incremental encoder. Since the incremental encoder gives a reliable measurement signal the drive speed may be calculated by discrete differentiation of the drive position. Further, a gyroscope may be installed at the hook, in particular the hook housing, for measuring the inertial skewing rate of the hook. Said gyroscope measurement may be disturbed by a signal bias and a sensor noise. The slewing angle of the crane may be measured by another sensor, for instance an incremental encoder installed at the slewing gear.

[0025] Furthermore, the rope length may be measured precisely and a spreader length used for grabbing a container may be derived from a spreader actuation signal. It may be possible to calculate the radius of gyration from the spreader length.

[0026] A good quality for estimation of the system state is achieved by using a state observer of a Luenberger-type. However, any other type of a state observer may be applicable.

[0027] The state observer may be implemented without the use of a Kalman filter since the model for characterizing the skew dynamic is independent of the load mass and/or the moment of inertia of the load mass.

[0028] As described before, the systems known from DE 100 29 579 and DE 10 2006 033 277 A1 employ a state observer which needs the second derivative of a position measurement. Such a double differentiation is disadvantageous due to noise amplification. According to preferred aspect of the present invention the used coordinate system for describing the state of the system has been changed to an extent that the present invention does not require double differentiation.

[0029] It is advantageous when the reference trajectory generator calculates a nominal state trajectory and/or a nominal input trajectory which is/are consistent with the crane dynamics, i.e. skew dynamics and/or rotator drive dynamics and/or measured crane tower motion. Consistency with skew dynamics means that the reference trajectory fulfills the differential equation of the skew dynamics and does not violate skew deflection constraints. Consistency with drive dynamics means that the reference trajectory fulfills the differential equation of the drive dynamics and violates neither drive velocity constraints nor drive torque constraints.

[0030] A generation of the nominal state and input trajectory is preferable performed by using the non-linear model for the skew dynamics. That is to say that a simulation of the non-linear skew dynamic model and/or a simulation of the rotator unit model is/are implemented at the reference trajectory generator for calculation of a nominal state trajectory and/or a nominal input trajectory consistent with the aforementioned crane dynamics.

[0031] Further preferable a disturbance decoupling block of the reference trajectory generator decouples the skewing dynamics from the crane's slewing dynamics. That is to say that the slewing gear can still be manually controlled by the crane operator during an active skew control. The same may apply to the dynamics of the luffing gear. Consequently, the control of the skewing angle may be decoupled from the slewing gear and/or the luffing gear of the crane.

[0032] In a particular preferred embodiment of the present invention the reference trajectory generator enables an operator triggered semi-automatic rotation of the load of a predefined angle, in particular of about 90° and/or 180°. That is to say the control unit offers certain operator input options which will proceed an semi-automatically rotation/skew of the attached load for a certain angle, ideally 90° and/or 180° in a clockwise and/or counter-clockwise direction. The operator may simply push a predefined button on a control stick to trigger an automatic rotation/skew of the load wherein the active skew control of the skew unit avoid torsional oscillations during skew movements.

[0033] The present invention is further directed to a skew control system for controlling the orientation of a crane load using any one of the methods described above. Such a skew control unit may include a 2-DOF control for the skew angle. The skew control system may include a reference trajectory generator and/or a state observer and/or a control unit for controlling the control signal of a rotator unit and/or slewing gear and/or luffing gear.

[0034] The present invention further comprises a boom crane, especially a mobile harbour crane, comprising a skew control unit for controlling the rotation of a crane load using any of the methods described above. Such a crane comprises a hook suspended on ropes, a rotator unit and a manipulator.

[0035] Advantageously, the crane will also comprise an anti-sway-control system that interacts with the system for controlling the rotation of a crane. The crane may also comprise a boom that can be pivoted up and down around a horizontal axis and rotated around a vertical axis by a tower. Additionally, the length of the rope can be varied.

[0036] Further advantages and properties of the present invention are described on the basis of embodiments shown in the figures. The figures show:

- Fig. 1: shows a side view and a top view of a mobile harbour crane,
- Fig. 2: a front view of the crane ropes, load rotator device, spreader and container,
- 50 Fig. 3: an overview of the different operating modes for rotator control during container transloading,
 - Fig. 4: a side view of a joystick with hand lever buttons for skew control,
 - Fig. 5: a top view of the geometry and variables of the skew dynamics model,
 - Fig. 6: an illustration of the cuboid model of the load,

10

20

30

35

40

45

55

Fig. 7: a sketch of the boom tip, ropes and hook in a deflected situation,

- Fig. 8: a side view of a crane hook with installed components,
- Fig. 9: a schematic for the two-degree of freedom control for the skew angle,
- Fig. 10: a diagram disclosing the closed-loop stability region,
 - Fig. 11: a signal flow chart for determining the target speed,
 - Fig. 12: measurement result of a slewing gear rotation of 90° and
 - Fig. 13: measurement results to demonstrate the usage of the semi-automatic container turning function.

[0037] Boom cranes are often used to handle cargo transshipment processes in harbours. Such a mobile harbour crane is shown in Fig. 1. The crane has a load capacity of up to 124t and a rope length of up to 80m. However, the invention is not restricted to a crane structure with the mentioned properties. The crane comprises a boom 1 that can be pivoted up and down around a horizontal axis formed by the hinge axis 2 with which it is attached to a tower 3. The tower 3 can be rotated around a vertical axis, thereby also rotating the boom 1 with it. The tower 3 is mounted on a base 6 mounted on wheels 7. The length of the rope 8 can be varied by winches. The load 10 can be grabbed by a manipulator or spreader 20, that can be rotated by a rotator unit 15 mounted in a hook suspended on the rope 8. The load 10 is rotated either by rotating the tower and thereby the whole crane, or by using the rotator unit 15. In practice, both rotations will have to be used simultaneously to orient the load in a desired position.

[0038] Figure 2 discloses a detailed side view of a container 10 grabbed by the spreader 20. The spreader 20 is attached to the hook 30 by means of hinge 31 which is rotatable relative to the hook 30. The hook 30 is attached to the ropes 8 of the crane. A detailed view of the hook 30 is depicted in Figure 8. The rotator unit effecting a rotational movement of the attached spreader relative to the hook 30 comprises a drive including rotator motor 32 and transmission unit 33. A power line 37 connects the motor 32 to the power supply of the crane. The hook 30 further comprises an inertial skew rate sensor 34 (gyroscope) and a drive position sensor 35 (incremental encoders). A spreader can be connected to the attaching means 38.

[0039] For simplicity, only the rotation of a load suspended on an otherwise stationary crane will be discussed here. However, the control concept of the present invention can be easily integrated in a control concept for the whole crane. [0040] The present invention presents the skew dynamics on a boom crane along with an actuator model and a sensor configuration. Subsequently a two-degrees of freedom control concept is derived which comprises a state observer for the skew dynamics, a reference trajectory generator, and a feedback control law. The control system is implemented on a Liebherr mobile harbour crane and its effectiveness is validated with multiple test drives.

[0041] The novelties of this publication include the application of a nonlinear skew dynamics model in a 2-DOF control system on boom cranes, the real-time reference trajectory calculation method which supports operating modes such as perpendicular transfer of containers, and the experimental validation on a harbour cranes with a load capacity of 124 t.

2 Rotator Operation Modes

10

15

20

30

35

40

45

50

55

[0042] In this section, typical operating modes for container rotation during container transloading are discussed.

[0043] In most harbours, containers 10 are moved from a container vessel 40 to shore 50 without rotation. This is commonly called parallel transfer; see Figure 3(a). On thin piers 51 ("finger piers") however, containers 10 need to be rotated by 90° to allow further transport using reach stackers. Such a perpendicular transfer is depicted in Figure 3(b). When containers 10 are transferred to trucks or automated guided vehicles (AGVs) (reference number 41), the crane must precisely adjust the container skew angle to the truck orientation. Since container doors 11 must be at the rear end of a truck 41, containers 10 are sometimes turned by 180°. These processes are shown in Figure 3(c).

[0044] Figure 4 shows one of the hand levers of the crane operator. Two hand lever buttons 60, 61 are used for adapting the spreader orientation in either clockwise direction by pushing button 60 or counterclockwise direction by pushing button 61. The state of the art is that pushing one of these buttons induces a relative motion between the hook and the spreader in the desired direction. When no button is pressed, either the relative velocity between hook and spreader is forced to zero, or the actuator is set to zero-torque. In both cases the load motion will not stop when the operator releases the hand lever buttons, but either an undamped residual oscillation of the spreader will remain, or the spreader will remain in constant rotation. In both cases the operator has to compensate disturbances due to wind, crane slewing motion, friction forces, etc. himself.

[0045] When automatic skew control is enabled on a crane, the same user interface shall be used. This means that the operator shall control the spreader motion using only the two hand lever buttons. When there is no operator input, the skew angle shall be kept constant to allow parallel transfer of containers. This means that both known disturbances

(e. g. slewing motion) and unknown disturbances (e. g. wind force) need to be compensated. Short-time button pushes shall yield small orientation changes to allow precise positioning. When a button is kept pushed for longer periods, the container is accelerated to a constant target speed, and it is decelerated again once the button is released. The target speed is chosen such that the braking distance is sufficiently small to ensure safe working conditions (the braking distance shall not exceed 45°). To simplify perpendicular transfer of containers or 180° container rotation, the skewing motion shall automatically stop at a given angle (90° or 180°) even if the operator keeps the button pressed.

3 Crane Rotator Model

[0046] According to the invention a dynamic model for the skew angle is derived. As shown in Figure 5, the skew angle of the load in inertial coordinates is referred to as η_L . The load can be an empty spreader 20 or a spreader 20 with a container 10 hooked onto it. The slewing angle of the crane is denoted as φ_D , and the relative angle between the rotator device and the load is φ_C . The directions of the angles are defined as shown in Figure 5. Subsection 3.1 introduces a dynamic model of the skew dynamics, i. e. a differential equation for the skew angle η_L . A drive model for the rotator angle φ_C is given in Subsection 3.2. Finally, the available sensor signals are presented in Subsection 3.3.

3.1 Load Rotation Dynamics

20

25

35

40

45

[0047] In this section, a model for the oscillation dynamics of the inertial skew angle η_L is derived. The Figures 2, 5 and 6 visualize the angles and lengths appearing in the derivation.

[0048] The spreader (with or without a container) is assumed to be a uniform cuboid of dimensions $k_1 \times k_2 \times k_3$ with the mass m_L (see Figure 6). The cuboid's inertia tensor is then

$$\mathbf{I} = \frac{1}{12} m_L \begin{bmatrix} k_2^2 + k_3^2 & 0 & 0\\ 0 & k_1^2 + k_3^2 & 0\\ 0 & 0 & k_1^2 + k_2^2 \end{bmatrix}.$$
 (1)

[0049] With the vertical position h_L , the horizontal position x_L , y_L and the rotation rates $\dot{\beta}$, $\dot{\gamma}$, $\dot{\delta}$, and the gravitational acceleration g, the potential energy v and the kinetic energy Tof the container are:

$$V = m_L g h_L, \tag{2}$$

$$\mathcal{T} = \frac{1}{2} m_L \left[\dot{h}_L^2 + \dot{x}_L^2 + \dot{y}_L^2 \right] + \frac{1}{2} \left[\dot{\beta} \ \dot{\gamma} \ \dot{\delta} \right] \mathbf{I} \begin{bmatrix} \dot{\beta} \\ \dot{\gamma} \\ \dot{\delta} \end{bmatrix}
= \frac{1}{2} m_L \left[\dot{h}_L^2 + \dot{x}_L^2 + \dot{y}_L^2 \right] + \frac{1}{24} m_L \left[(k_2^2 + k_3^2) \dot{\beta}^2 + (k_1^2 + k_3^2) \dot{\gamma}^2 + (k_1^2 + k_2^2) \dot{\delta}^2 \right].$$
(3)

[0050] Both (2) and (3) are combined to the Lagrangian $\mathcal{L} = \mathcal{T} - \mathcal{V}$. In order to apply the Euler-Lagrange equation

$$\frac{\mathrm{d}}{\mathrm{d}t}\frac{\partial \mathcal{L}}{\partial \dot{\eta}_L} = \frac{\partial \mathcal{L}}{\partial \eta_L},\tag{4}$$

[0051] it must be identified which terms in (2) and (3) depend on either the skew angle η_L or its derivative $\dot{\eta}_L$:

- The vertical load position h_L depends on η_L : When the container rotates around the vertical axis, it is slightly lifted upwards due to the cable suspension. The exact dependency is derived in the following.
 - Since a rotation of the load does not move the center of gravity of the load horizontally, the horizontal load position coordinates x_L and y_L do not depend on η_L .

• In typical crane operating conditions, the load angles γ and δ are very small. This means that the angle β coincides with the container orientation η_I . Since γ and δ are orthogonal to β , they do not depend on η_I .

[0052] The Lagrangian can therefore be represented as:

$$\mathcal{L} = \frac{1}{2} m_L \dot{h}_L^2 + \frac{1}{24} m_L \underbrace{\left(k_2^2 + k_3^2\right)}_{k_L^2} \dot{\eta}_L^2 - m_L g h_L. \tag{5}$$

[0053] In order to apply (4) to (5), the relative load height h_L needs to be written as a function of the rotator deflection (i. e. the twist angle $\Diamond = \eta_L - \varphi_C - \varphi_D$). Figure 7 shows the rotator in a deflected state. The cosine formula for the triangle A is:

$$s_x^2 = \left(\frac{s_a}{2}\right)^2 + \left(\frac{s_b}{2}\right)^2 - 2\frac{s_a}{2}\frac{s_b}{2}\cos\left(\eta_L - \varphi_C - \varphi_D\right). \tag{6}$$

[0054] With S_x known, geometric considerations in triangle B reveal

$$-h_L = \sqrt{L^2 - s_x^2},\tag{7}$$

which yields:

5

10

25

35

45

50

55

$$h_L = -\sqrt{L^2 - \frac{s_a^2}{4} - \frac{s_b^2}{4} + \frac{s_a s_b}{2} \cos(\eta_L - \varphi_C - \varphi_D)}.$$
 (8)

[0055] Using (5) and (8), the Euler-Lagrange formalism (4) yields the differential equation (9) which describes the skew dynamics.

$$k_{L}^{2}m_{L}\ddot{\eta}_{L} + \frac{m_{L}s_{a}^{2}s_{b}^{2}\xi_{2}^{2}}{4\xi_{1}} \left(\ddot{\eta}_{L} - \ddot{\varphi}_{C} - \ddot{\varphi}_{D} \right) = -\underbrace{\frac{m_{L}s_{a}^{2}s_{b}^{2}\xi_{2}\xi_{4}^{2}}{4\xi_{1}}}_{\star} \left(\frac{s_{a}s_{b}\xi_{2}^{2}}{\xi_{1}} + \xi_{3} \right) - \underbrace{\frac{m_{L}gs_{a}s_{b}\xi_{2}}{2\sqrt{\xi_{1}}}}_{\star}$$
(9a)

40 with

$$\xi_1 = 4L^2 - s_a^2 - s_b^2 + 2s_a s_b \xi_3 \tag{9b}$$

$$\xi_2 = \sin\left(\eta_L - \varphi_C - \varphi_D\right) \tag{9c}$$

$$\xi_3 = \cos\left(\eta_L - \varphi_C - \varphi_D\right) \tag{9d}$$

$$\xi_4 = \dot{\varphi}_C + \dot{\varphi}_D - \dot{\eta}_L \tag{9e}$$

[0056] The following assumptions are used to simplify equation (9):

• The rope distances are significantly smaller than the rope length: $s_a << L$, $s_b << L$.

- The term marked as * can be neglected when being compared with the term marked as \blacksquare : Even for short rope lengths ($L_{\min} \approx 5$ m) and high rotational rates ($|\xi_4|_{\max} \approx 0.8^{\text{rad}}/\text{s}$), $\frac{s_a s_b}{L} \xi_4^2 \leq \frac{s_a s_b}{L_{\min}} |\xi_4|_{\max}^2 \approx 0.5^{\text{m}}/\text{s}^2 \ll g$ holds.
- Due to the rotational inertia which is represented by the radius of gyration k_L which was defined in (5), the translational inertia is negligible:

$$\frac{1}{16} m_L \frac{s_a^2 s_b^2}{L^2} \ll m_L k_L^2$$

5

15

25

40

50

[0057] With these assumptions, the skew dynamics (9) can be denoted as

$$m_L k_L^2 \ddot{\eta}_L = \underbrace{-m_L \frac{g}{L} \frac{s_a s_b}{4} \sin\left(\eta_L - \varphi_C - \varphi_D\right)}_{T}. \tag{10}$$

[0058] The right-hand side of (10) is the torque Texerted on the load. The product of the halve rope distances is abbreviated as

$$A = \frac{s_a s_b}{4} \tag{11}$$

which is a parameter that is known from the crane geometry. Combining (10) and (11) yields the skew dynamics model

$$\ddot{\eta}_L = -\frac{g}{L} \frac{A}{k_L^2} \sin\left(\eta_L - \varphi_C - \varphi_D\right). \tag{12}$$

[0059] Equation (12) illustrates that the eigenfrequency of the skew dynamics is independent of the load mass, i. e. only depends on the geometry and on the gravitational acceleration. Also, (12) illustrates that it is not reasonable to leave the deflection range

$$-\frac{\pi}{2} \le \eta_L - \varphi_C - \varphi_D \le \frac{\pi}{2} \tag{13}$$

since larger deflections do not yield higher torques.

3.2 Actuator Model

[0060] The skewing device rotates the spreader with respect to the hook (see Figure 8). The relative angle is denoted as $\varphi_{\mathbb{C}}$. If the rotator is hydraulically actuated the control signal u can be a valve position which is proportional to the rotator speed. If the rotator is electrically actuated the control signal u can be a rotation rate set-point. Assuming first-order lag dynamics with a time constant $T_{S'}$ the actuator dynamics can be denoted as:

$$T_S\ddot{arphi}_C + \dot{arphi}_C = u.$$
 (14)

[0061] The actuator system is subject to two contraints. First, the control signal u cannot exceed given limits:

$$u_{\min} \le u \le u_{\max}. \tag{15}$$

[0062] Second, the drive system is limited in torque and/or pressure and/or current, therefore only a certain skew torque T_{max} can be applied by the actuators. Considering (10), the skew torque constraint is:

$$\left| m_L \frac{g}{L} A \sin \left(\eta_L - \varphi_C - \varphi_D \right) \right| \le T_{\text{max}}. \tag{16}$$

[0063] This constraint is important for trajectory generation since the system will inevitably deviate from the reference trajectory if the constraint is violated.

3.3 Sensor Models

15

20

25

30

35

40

45

50

55

10 [0064] There are two sensors installed in the hook housing (see Figure 8). An incremental encoder is used for measuring the drive position

$$y_1 = \varphi_C. \tag{17}$$

[0065] Since the incremental encoder gives a reliable measurement signal, the drive speed $\dot{\varphi}_C$ is found by discrete differentiation of the drive position. For measuring the skew dynamics, a gyroscope is installed in the hook housing, which measures its inertial skewing rate. The gyroscope measurement is disturbed by a signal bias and sensor noise:

$$y_2 = \dot{\eta}_L - \dot{\varphi}_C + \nu_{\text{offset}} + \nu_{\text{noise}}. \tag{18}$$

[0066] The slewing angle of the crane is also measured by an incremental encoder (see Figure 5):

$$y_3 = \varphi_D. (19)$$

[0067] Furthermore the rope length L of the crane is measured precisely, and the spreader length $I_{\rm spr}$ is known from the spreader actuation signal (see Figure 2). From the spreader length, the radius of gyration k_L can be calculated. For calculating the radius of gyration, the following parts have to be taken into account:

- the crane hook, which however gives very little rotational inertia,
- the empty spreader, which has a length-dependent mass distribution that is known from the spreader manufacturer,
- if attached, the steel container, whose (length-dependent) mass distribution is known from identification experiments,
- if present, the load inside the container, which is simply assumed to be equally distributed over the (length-dependent) container floor space.

[0068] The crane's load measurement is only used to decide if the container has to be taken into account for the calculation of the radius of gyration k_I .

4 Control Concept

[0069] For the skew control, two-degree of freedom control is used as shown in Figure 9. This means that the control signal u comprises a feedforward signal \tilde{u} from a reference trajectory generator, and a feedback signal Δ_u to stabilize the system and reject disturbances:

$$u = \tilde{u} + \Delta u. \tag{20}$$

[0070] The feedforward control signal \tilde{u} is designed in such a way that it drives the system along a reference trajectory \tilde{x} under nominal conditions. Any deviation of the estimated system state \tilde{x} to the reference state \tilde{x} is compensated by the feedback signal Δu using the feedback gain vector k^{T} :

$$\Delta u = k^{\mathsf{T}} \left(\tilde{x} - \hat{x} \right). \tag{21}$$

[0071] The system state x comprises the rotator angle φ_C , rotator angular rate $\dot{\varphi}_C$, the skew angle η_L and the skew

angular rate $\dot{\eta}_L$:

$$x = \begin{bmatrix} \varphi_C \\ \dot{\varphi}_C \\ \eta_L \\ \dot{\eta}_L \end{bmatrix} .$$
 (22)

[0072] In Section 4.1, a state observer is presented which finds the state estimate \hat{x} for the real system state x using the measurement signals. The design of the feedback gain k^T is discussed in Section 4.2. Finally, the reference trajectory generator which calculates \tilde{u} and \tilde{x} is shown in Section 4.3.

4.1 State Observer

15

20

25

30

40

50

[0073] The aim of the state observer is to estimate those states of the state vector (22) which cannot be measured or whose measurements are too disturbed to be used as feedback signals. Both states of the actuator dynamics are measured using an incremental encoder. This means that φ_C and φ_C are known and do not need to be estimated. The two states of the skew dynamics, the skew angle η_L and its angular velocity $\dot{\eta}_L$, are not directly measurable. They are estimated using a Luenberger-type state observer. The gyroscope measurement (18) is used as feedback signal for the observer. Since the gyroscope measurement carries a signal offset v_{offset} , an augmented observer model is introduced for observer design, i. e. the observer state vector z_{s} comprises the skew angle η_L , the skew rate $\dot{\eta}_L$ and the signal offset v_{offset} and the skewing rate v_{spiel} caused by the slackness of the hook and the time derivative \dot{v}_{spiel} thereof:

$$\boldsymbol{z}_{\mathbf{S}} = \begin{bmatrix} z_1 \\ z_2 \\ z_3 \\ z_4 \\ z_5 \end{bmatrix} = \begin{bmatrix} \eta_{\mathbf{L}} \\ \dot{\eta}_{\mathbf{L}} \\ \nu_{\text{offset}} \\ \nu_{\text{spiel}} \\ \dot{\nu}_{\text{spiel}} \end{bmatrix}. \tag{23}$$

[0074] The nominal dynamics of z_s are found by combining (12) with a random-walk offset model:

$$\dot{z}_{S} = \begin{bmatrix}
-\frac{g}{L} \frac{A}{k_{L}^{2}} \sin (z_{1} - \varphi_{C} - \varphi_{D}) \\
0 \\
z_{5} \\
-\left(\frac{2\pi}{k_{S}}\right)^{2} z_{4}
\end{bmatrix}, \tag{24a}$$

$$y_2 = z_2 - \dot{\varphi}_C + z_3 + z_4. \tag{24b}$$

[0075] The observer is found by adding a Luenberger term to (24). The estimated state vector is denoted as \hat{z}_s . The signals φ_C , φ_D , and $\dot{\varphi}_C$ are taken from the measurements (17) and (19):

$$\hat{\boldsymbol{z}}_{S} = \begin{bmatrix}
-\frac{g}{L} \frac{A}{k_{L}^{2}} \sin(\hat{z}_{1} - y_{1} - y_{3}) \\
0 \\
\hat{z}_{5} \\
-\left(\frac{2\pi}{l_{18}}\right)^{2} \hat{z}_{4}
\end{bmatrix} + \begin{bmatrix}
l_{1} \\
l_{2} \\
l_{3} \\
l_{4} \\
l_{5}\end{bmatrix} (y_{2} - \hat{y}_{2}), \tag{25a}$$

$$\hat{y}_2 = \hat{z}_2 - \hat{y}_1 + \hat{z}_3 + \hat{z}_4. \tag{25b}$$

[0076] The feedback gains l_1 , l_2 , l_3 , l_4 and l_5 are found by pole placement to ensure required convergence times after

situations with model mismatch. A typical example for model mismatch is a collision with a stationary obstacle (e. g. another container). For the pole placement procedure, a set-point linearization of the observer model is used.

[0077] From the estimated state vector \hat{z}_s , the estimated skew angle and the skew rate are forwarded to the 2-DOF control, along with the actuator state measurements. The estimated gyroscope offset is not considered further:

 $\hat{x} = \begin{bmatrix} y_1 \\ \dot{y}_1 \\ \dot{z}_1 \\ \dot{z}_2 \end{bmatrix} . \tag{26}$

4.2 Stabilization

5

10

20

25

30

35

40

45

50

55

[0078] Since both the skew dynamics (12) and the actuator dynamics (14) have open loop poles on the imaginary axis, any disturbance (e. g. wind) or error in the initial state estimate will cause non-vanishing deviations in between the reference trajectory \tilde{x} and the system trajectory x. Feedback control is added to ensure that the system converges to the reference trajectory (see Figure 9). The feedback control is accomplished by calculating the control error

$$e = \tilde{x} - x \tag{27}$$

and designing the feedback gain k^{T} with

$$k^{\top} = \begin{bmatrix} k_1 & k_2 & k_3 & k_4 \end{bmatrix} \tag{28}$$

for eq. (21) such that the control error is asymptotically stable. For the feedback design, a set-point linearization is considered. Afterwards it is verified that the feedback law stabilizes the nonlinear system model.

[0079] Assuming both the reference trajectory and the plant dynamics fulfill the model equations (12) and (14), the error dynamics can be found by differentiating (27) and plugging-in the model equations:

$$\dot{e} = \dot{\tilde{x}} - \dot{x} = \begin{bmatrix}
\tilde{x}_{2} \\
-\frac{1}{T_{S}}(\tilde{x}_{2} - \tilde{u}) \\
\tilde{x}_{4} \\
-\frac{gA}{Lk_{L}^{2}}\sin(\tilde{x}_{3} - \tilde{x}_{1})
\end{bmatrix} - \begin{bmatrix}
x_{2} \\
-\frac{1}{T_{S}}(x_{2} - u) \\
x_{4} \\
-\frac{gA}{Lk_{L}^{2}}\sin(x_{3} - x_{1})
\end{bmatrix}.$$
(29)

[0080] Together with the control equations (20), (21), and (28), and assuming the state estimation works sufficiently well $(\hat{x} = x)$, the set-point linearization of (29) is

$$\dot{e} = \underbrace{\begin{bmatrix} 0 & 1 & 0 & 0 \\ -\frac{k_1}{T_S} & -\frac{1+k_2}{T_S} & -\frac{k_3}{T_S} & -\frac{k_4}{T_S} \\ 0 & 0 & 0 & 1 \\ \frac{g}{L} \frac{A}{k_L^2} & 0 & -\frac{g}{L} \frac{A}{k_L^2} & 0 \end{bmatrix}}_{\Phi} e.$$
(30)

[0081] With the abbreviation $\theta=rac{g}{L}rac{A}{k_L^2}$, the characteristic polynomial of the dynamic matrix Φ is:

$$\det(\lambda I - \Phi) = \frac{(k_1 + k_3)\theta + (k_2 + k_4 + 1)\theta\lambda + (k_1 + T_S\theta)\lambda^2 + (k_2 + 1)\lambda^3 + T_S\lambda^4}{T_S}$$
(31)

[0082] For any parameters θ and T_S , the feedback gains $k_1,...k_4$ can be chosen in such a way that (31) is a Hurwitz polynomial. The final feedback gains can be chosen by various methods. A graphical tool are stability plots. For example, the stability region for $k_2 = k_3 = 0$ is depicted in Figure 10, which shows the constraints on the choice for the remaining coefficients k_1 und k_4 for this case.

10 4.3 Reference Trajectory Generation

15

20

25

30

40

45

[0083] As shown in Figure 9, the reference trajectory generator needs to calculate a nominal state trajectory \tilde{x} as well as a nominal input trajectory \tilde{u} which is consistent with the plant dynamics. Since the skew system is operator-controlled, the reference trajectory needs to be planned online in real-time.

[0084] The general structure is known which uses a plant simulation to generate a reference state trajectory and an arbitrary control law for generating a control input for the plant simulation. The control input for the simulated plant is then used as a nominal control signal for the real system. In order to adapt this approach to the skew control problem, simulations of the actuator model and the skew model are implemented for generating a reference state trajectory from a reference input signal. In this design, the combined angle

$$\tilde{\varphi}_{CD} = \tilde{\varphi}_C + \varphi_D \tag{36}$$

is used instead of the actuator angle φ_C and the slewing gear angle φ_D at first. The two variables are later decoupled as discussed in Section 4.3.3. The remainder of this section discusses the control law which is used to stabilize the plant simulation. Since the cut-off frequency of the actuator dynamics is significantly faster than the eigenfrequency of the skew dynamics, cascade control is applied inside the reference trajectory planner. This means that a skew reference controller is set up for stabilizing the simulated skew dynamics, and an underlying actuator reference controller is used

for stabilizing the simulated actuator dynamics. The target value of the skew control loop is the target velocity $\tilde{\eta}_{L,\text{target}}$ from the operator, and the target value of the underlying actuator control loop comes from the skew control loop. A disturbance decoupling block is added to decouple the skewing dynamics from the crane's slewing dynamics, i. e. reverting (36). Finally, the automatic deceleration at position constraints after 90° or 180° of motion are enforced by modification of the target velocity for the whole reference control loop.

[0085] The skew reference control loop is explained in Subsection 4.3.1, followed by the actuator reference control loop in Subsection 4.3.2. Subsequently, the decoupling of the slewing gear motion is shown in Subsection 4.3.3. Finally, the determination of the target velocity is discussed in Subsection 4.3.4.

4.3.1 Skew Reference Controller

[0086] The aim of the skew reference controller is to stabilize the skew dynamics simulation

$$\ddot{\tilde{\eta}}_L = -\frac{gA}{Lk_L^2} \sin\left(\tilde{\eta}_L - \tilde{\varphi}_{CD}\right) \tag{37}$$

and to ensure that it tracks the target velocity $\hat{ ilde{\eta}}_{L, {
m target}}$. For this purpose the control law

$$\tilde{\varphi}_{CD,\text{target}} = \tilde{\eta}_L + \text{sat}_{\eta} \left(K_{\eta} \cdot \left(\dot{\tilde{\eta}}_{L,\text{target}} - \dot{\tilde{\eta}}_L \right) \right) \tag{38}$$

is introduced with the saturation function

$$\operatorname{sat}_{\eta}(x) = \operatorname{sign}(x) \cdot \min\left(\Delta \eta_{\max}, \arcsin\left(\frac{LT_{\max}}{qAm_L}\right), |x|\right). \tag{39}$$

[0087] The saturation function ensures that the target rope deflection neither exceeds the deflection which corresponds to maximum actuator torque as in (16), nor the maximum deflection angle $\Delta \eta_{\text{max}}$. The maximum deflection $\Delta \eta_{\text{max}} < \frac{\pi}{2}$ ensures that the reference trajectory does not deflect the hook beyond the maximum torque angle as in (13), and that there is a reasonable safety margin in case of control deviation. Assuming $\tilde{\varphi}_{CD} \approx \tilde{\varphi}_{CD,\text{target}}$, the skew dynamics (37) with the control law (38) breaks down to

$$\ddot{\tilde{\eta}}_L = \frac{gA}{Lk_L^2} \sin\left(\operatorname{sat}_{\eta}\left(K_{\eta} \cdot \left(\dot{\tilde{\eta}}_{L,\text{target}} - \dot{\tilde{\eta}}_L\right)\right)\right) \tag{40}$$

[0088] A stability analysis of (40) reveals that for any positive K_{η} the load skew rate $\tilde{\eta}_L$ asymptotically converges to any constant target velocity $\tilde{\eta}_{L,\text{target}}$. The feedback gain K_{η} is chosen by gain scheduling in dependence of the skew eigenfrequency. It ensures quick convergence with minimum overshoot.

4.3.2 Actuator Reference Controller

10

15

25

35

40

50

55

20 [0089] The underlying control loop consists of the plant

$$\ddot{\tilde{\varphi}}_{CD} = \frac{\tilde{u}_{CD} - \dot{\tilde{\varphi}}_{CD}}{T_S} \tag{41}$$

and the actuator reference controller which is designed using the following model predictive control approach. The actuator reference controller is designed such that the cost function

$$\min_{\tilde{u}_{CD}(t)} \int_{0}^{T_{\text{predict}}} q_{\varphi} \left(\tilde{\varphi}_{CD} - \tilde{\varphi}_{CD, \text{target}} \right)^{2} + q_{\tilde{u}} \tilde{u}_{CD}^{2} + q_{s} s^{2} dt \tag{42}$$

is minimized. Here, $s \ge 0$ is a high-weighted slack variable which is introduced to ensure that the following set of input and state constraints is always feasible:

$$\tilde{u}_{CD}(t) \le u_{\max},$$
(43)

$$-\tilde{u}_{CD}(t) \le -u_{\min},\tag{44}$$

$$\tilde{\varphi}_{CD}(t) - s(t) \le \tilde{\eta}_L + \operatorname{sat}_{\eta}(\infty),$$
(45)

$$-\tilde{\varphi}_{CD}(t) - s(t) \le -\tilde{\eta}_L + \operatorname{sat}_{\eta}(\infty). \tag{46}$$

[0090] The input constraints (43)-(44) ensure that the valve limitations (15) are not violated. The state constraints (45)-(46) are used to prevent remaining overshot with respect to the hook deflection constraint (39).

[0091] The optimal control problem (42)-(46) is discretized and solved using an interior point method.

4.3.3 Disturbance Decoupling

[0092] So far, reference values for the combined angle $\tilde{\varphi}_{CD}$ were calculated. As defined in (36), $\tilde{\varphi}_{CD}$ comprises the rotator angle and the slewing gear angle. However, the reference trajectory planner needs to calculate a nominal trajectory

for the rotator angle $\tilde{\varphi}_C$ only. Since the crane's slewing gear motion is known to the crane control system, it can be easily decoupled using the following formulas:

$$\tilde{\varphi}_C = \tilde{\varphi}_{CD} - \varphi_D, \tag{47a}$$

$$\dot{\hat{\varphi}}_C = \dot{\hat{\varphi}}_{CD} - \dot{\varphi}_{D_7} \tag{47b}$$

$$\tilde{u} = \tilde{u}_{CD} - (\dot{\varphi}_D + T_S \ddot{\varphi}_D). \tag{47c}$$

[0093] Equation (47a) directly reverts (36). Equation (47b) is found by differentiating (47a), and (47c) is found by further differentiation, and applying the actuator model (14) as well as (41).

4.3.4 Determination of the Target Velocity

5

10

15

20

25

30

35

40

50

55

[0094] The operator can only push joystick buttons in an on/off manner to operate the skewing system, i. e. the hand lever signal is

$$\omega \in \{-1, 0, +1\}. \tag{48}$$

[0095] The target velocity $\hat{\tilde{\eta}}_{L,\text{target}}$ for the skew reference controller is found by multiplying the joystick button signal with a reasonable maximum speed:

$$\dot{\tilde{\eta}}_{L,\text{target}} = \dot{\tilde{\eta}}_{L,\text{max}} \cdot \omega. \tag{49}$$

[0096] When the operator keeps a joystick button pressed permanently, the target velocity $\tilde{\eta}_{L,\text{target}}$ is overwritten with 0at some point to stop the skewing motion. The time instant of starting to overwrite the joystick button with 0is chosen such that the systems comes to rest exactly at the desired stopping angle $\tilde{\eta}_{\text{stop}}$. The stopping angle $\tilde{\eta}_{\text{stop}}$ is chosen application dependently. For turning a container frontside back, $\tilde{\eta}_{\text{stop}}$ is chosen 180° after the starting point. To identify the right point in time for overwriting the hand lever signal with 0, a forward simulation of the trajectory generator dynamics is conducted in every sampling interval with a target velocity of 0, yielding a stopping angle prediction $\tilde{\eta}_{\text{pred}}$. When this prediction reaches the desired stopping angle $\tilde{\eta}_{\text{stop}}$, further motion is inhibited in this direction, i. e. (49) is replaced by:

$$\dot{\tilde{\eta}}_{L,\text{target}} = \begin{cases}
0 & \text{if } \omega > 0 \land \tilde{\eta}_{\text{pred}} \ge \tilde{\eta}_{\text{stop}} \\
0 & \text{if } \omega < 0 \land \tilde{\eta}_{\text{pred}} \le \tilde{\eta}_{\text{stop}} \\
\dot{\tilde{\eta}}_{L,\text{max}} \cdot \omega & \text{else.}
\end{cases}$$
(50)

[0097] For the sake of clarity, the full target speed determination signal flow is shown in Figure 11.

5 Experimental Validation

[0098] To validate the practical implementation of the presented skew control system, two experiments are presented in this section. These experiments were chosen to reflect typical operating conditions as discussed in Section 2. The experiments were conducted on a Liebherr LHM 420 boom crane.

5.1 Compensation of Crane Slewing Motion

[0099] When the containers can be moved from ship to shore at a constant skew angle, the most important feature

of the presented control system is the decoupling of the skew dynamics from the slewing gear. Figure 12 shows a measurement of a slewing gear rotation of 90°. It can be seen that the rotator device φ_C moves inversely to the slewing gear φ_D , yielding a constant container orientation η_L . The control deviation is small all the time. The control deviation plot especially shows that the residual sway converges to amplitudes << 1°when the system comes to rest.

5.2 Large Angular Rotation

[0100] To demonstrate the usage of the semi-automatic container turning function, another test drive is shown in Figure 13. The container orientation is shown in Figure 13a, the angular rate is shown in Figure 13b and the control deviation is plotted in Figure 13c. When the operator presses the rotation button at the situation marked as (α) , the rotator starts moving and twists the ropes. During the motion, the rotator speed equals the load speed. In the situation marked as (β) , the rotator moves in inverse direction and decelerates the load. The system comes to rest after 180° rotation, which corresponds to the choice of the stopping angle $\tilde{\eta}_{\text{stop}}$ during this test drive. The deceleration at (β) is initialized automatically even though the operator does not release the rotation button. At (γ) and (δ) , the same motion occurs in opposite direction.

6 Conclusion

5

10

15

20

30

35

40

45

50

55

[0101] A nonlinear model for the skew dynamics of a container rotator of a boom crane and a suitable control system for the skew dynamics have been presented. The control system is implemented in a two-degrees of freedom structure which ensures stabilization of the skew angle, decoupling of slewing gear motions and simplifies operator control. A linear control law is shown to stabilize the system by use of the circle criterion. The system state is reconstructed from a skew rate measurement using a Luenberger-type state observer. The reference trajectory for the control system is calculated from the operator input in real-time using a simulation of the plant model. The simulation comprises appropriate control laws which ensure that the reference trajectory tracks the operator signal and maintains system constraints. The performance of the control system is validated with test drives on a full-size mobile harbour boom crane.

Claims

1. Method for controlling the orientation of a crane load, wherein a manipulator for manipulating the load is connected by a rotator unit to a hook suspended on ropes and the skew angle ηL of the load is controlled by a control unit of the crane,

characterized in that,

the control unit is an adaptive control unit wherein an estimated system state of the crane system is determined by use of a nonlinear model describing the skew dynamics during operation.

- 2. The method according to claim 1 **characterized in that** the non-linearity of the model describing the skew dynamics refers to the non-linear relation between the load deflection angle and the resulting reactive torque.
- 3. The method according to any of the preceding claims **characterized in that** the non-linear model is independent on the load mass or the moment of inertia of the load mass.
- **4.** The method according to any of the preceding claims **characterised in that** the estimated system state includes the estimated skew angle and/or the velocity of the skew angle and/or one or more parasitic oscillations of the skew system, for instance caused by the slackness of the hook.
 - 5. The method according to any of the preceding claims characterized in that the control unit is based on a 2-degree of freedom control comprising the state observer for estimation of the system state, a reference trajectory generator for generation of a reference trajectory in response to a user input and a feedback control law for stabilization of the nonlinear skew dynamic model.
 - **6.** The method according to claim 5 **characterized in that** the state observer receives measurement data comprising at least the drive position of the rotator unit and/or the inertial skewing rate and/or the slewing angle of the crane.
 - 7. The method according to claim 5 and 6 **characterized in that** the state observer is a Luenberger-type state observer.
 - 8. The method according to any of claims 4 to 7 characterised in that the state observer is implemented without the

use of a Kalman filter.

5

10

15

20

25

30

35

40

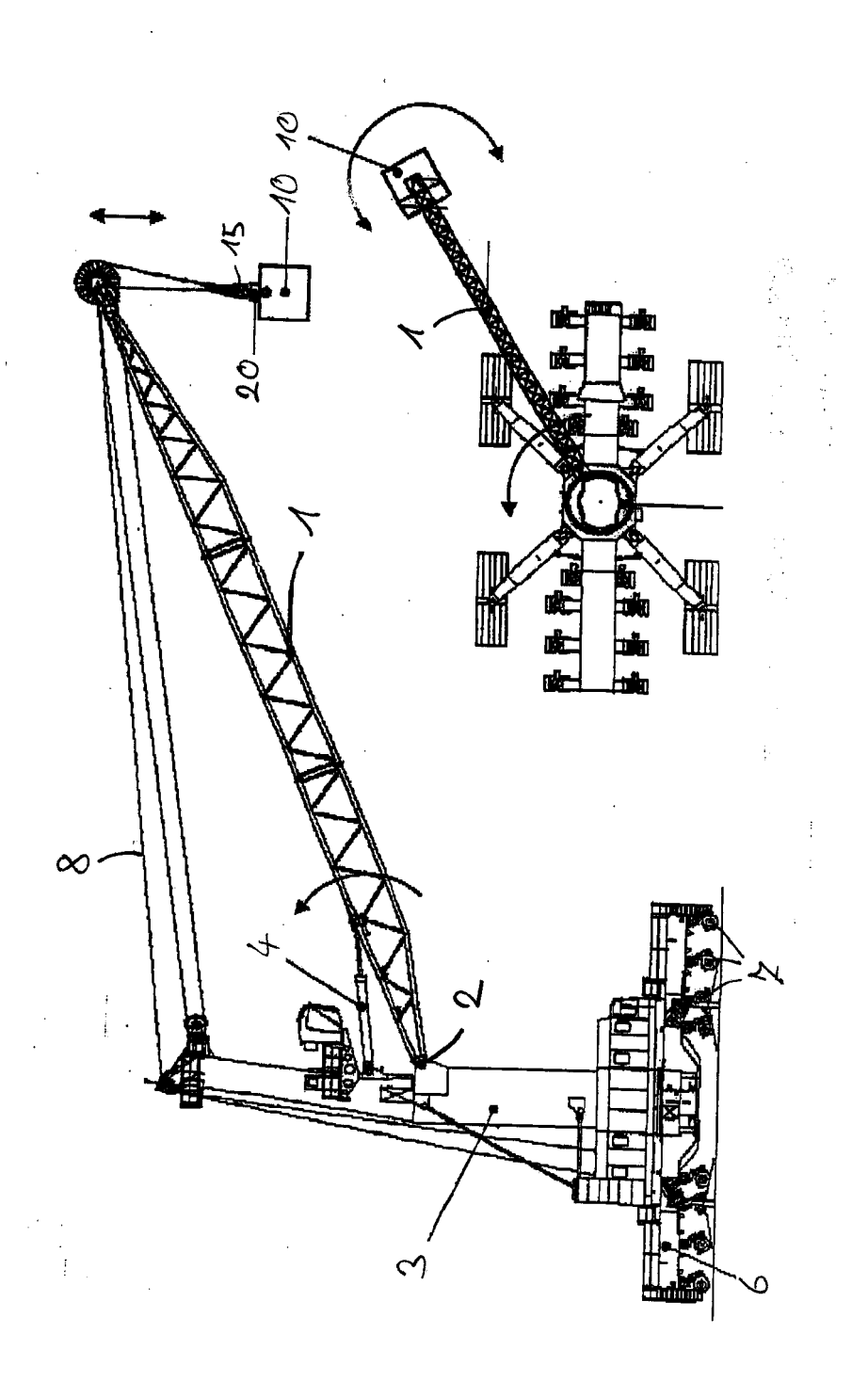
45

50

55

- **9.** The method according to any of claims 5 to 7 **characterised in that** the reference trajectory generator calculates a nominal state trajectory and/or a nominal input trajectory which is consistent with the skew dynamics and/or rotator drive dynamics and/or measured crane tower motion.
- **10.** The method according to any of claims 5 to 9 characterizing that a simulation of the non-linear skew dynamic model and/or a simulation of the rotator unit model is/are implemented at the reference trajectory generator for calculation of a nominal state trajectory and/or a nominal input trajectory consistent with the crane dynamics.
- **11.** The method according to any of claim 5 to 10 **characterized in that** a disturbance decoupling block of the reference trajectory generator decouples the skewing dynamics from the crane's slewing dynamics.
- **12.** The method according to any of the preceding claims 5 to 11 **characterized in that** the reference trajectory generator enables an operator triggered semi-automatic rotation of the load of a predefined angle, in particular of about 90° and/or 180°.
 - **13.** The method according to any of the preceding claims **characterized in that** the control of the skewing angle is decoupled from the slewing gear and/or the luffing gear of the crane.
 - **14.** A skew control system for a boom crane comprising means for performing the method according to any of the preceding claims.
 - 15. Boom crane, especially a mobile harbour crane, comprising a skew control system according to claim 14.

16



Fig

Fig. 2

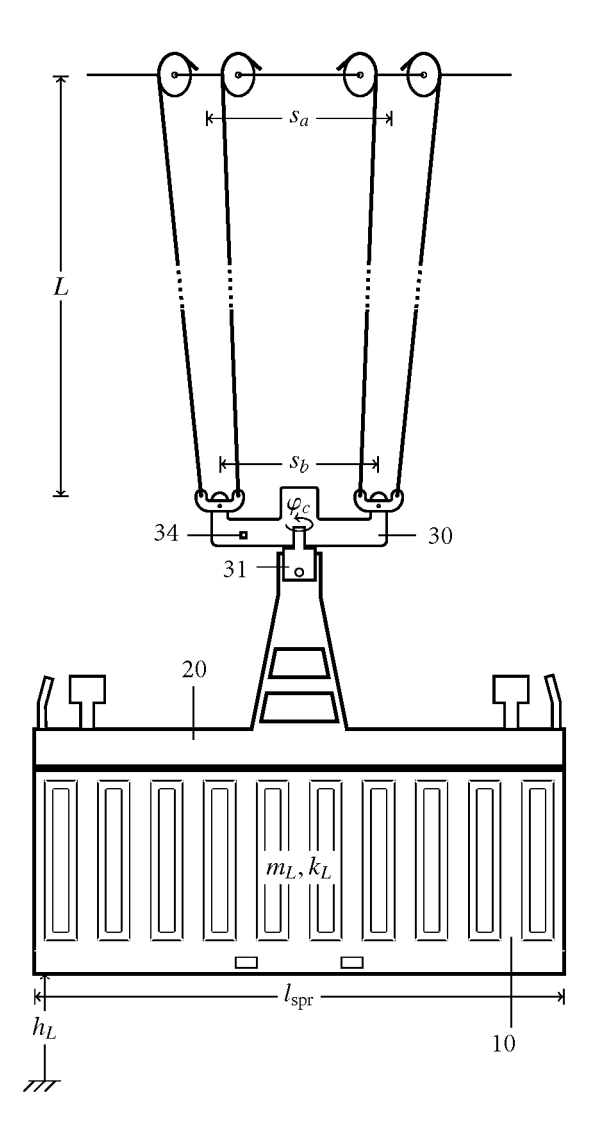
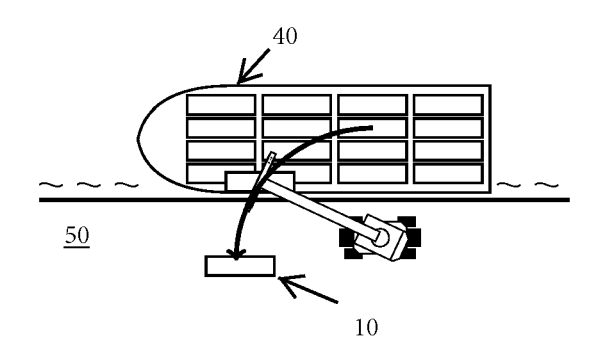


Fig. 3a



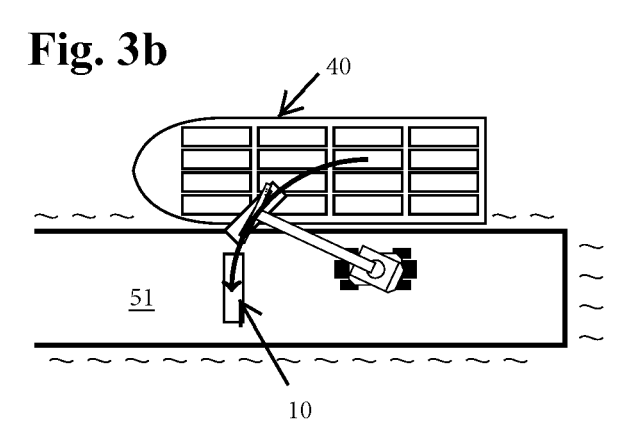
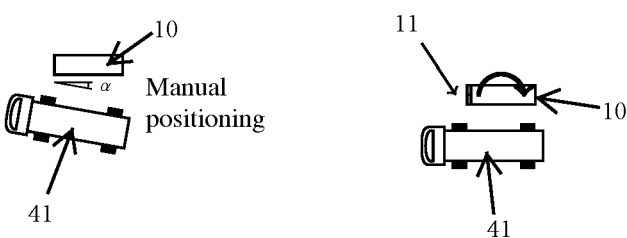
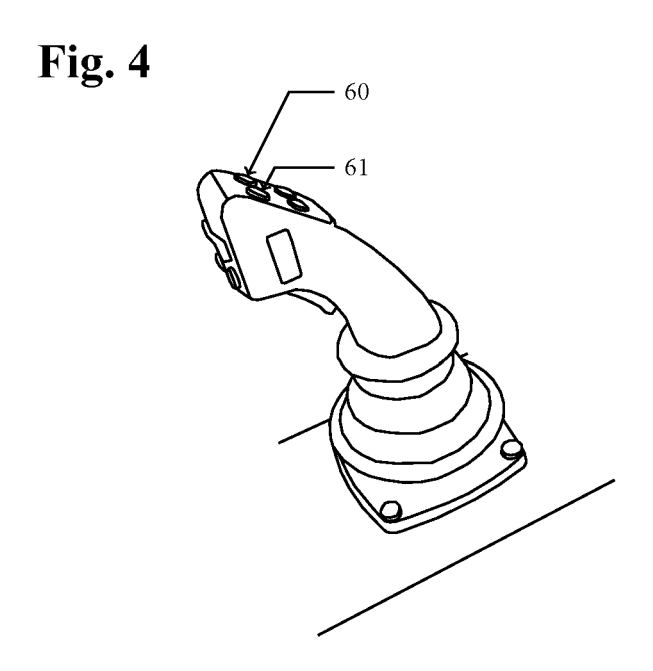
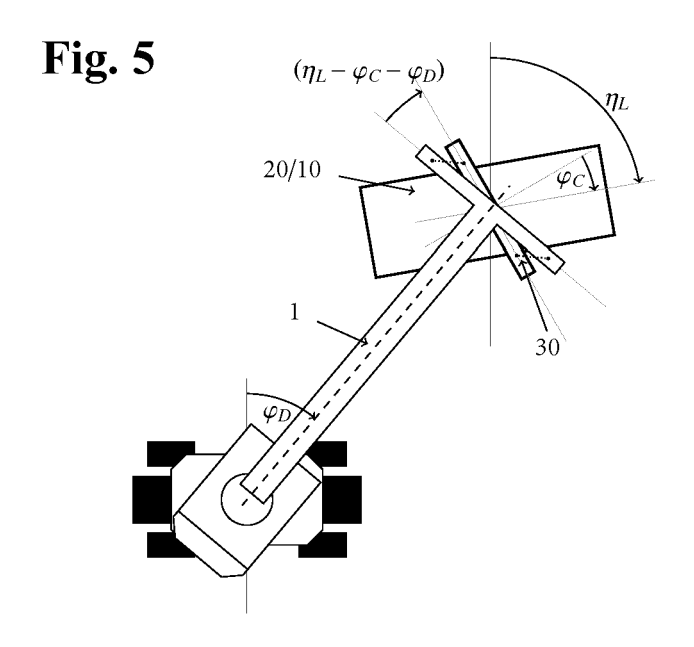


Fig. 3c









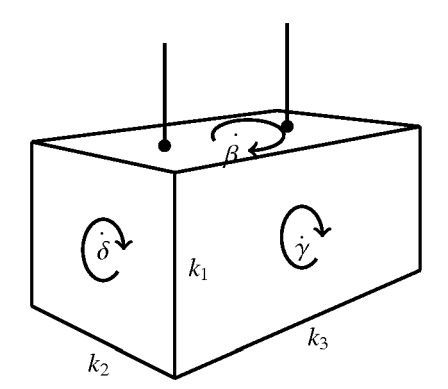


Fig. 7 boom tip center $\frac{1}{2}s_a$ $-h_L$ Bundeflected rotator orientation $\frac{1}{2}s_b$ real rotator orientation hook center

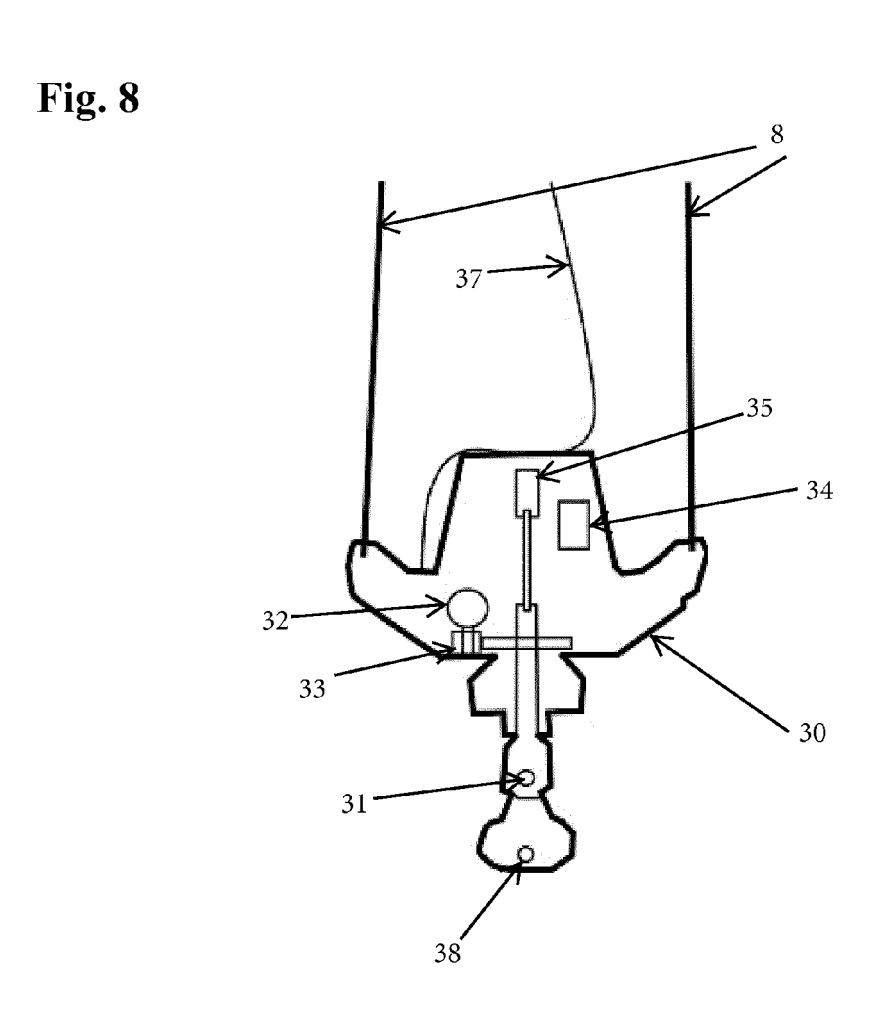


Fig. 9

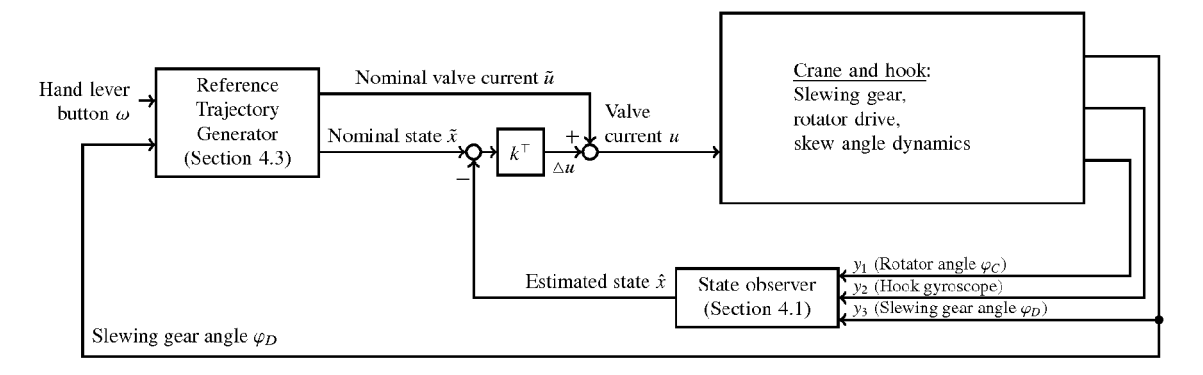


Fig. 10

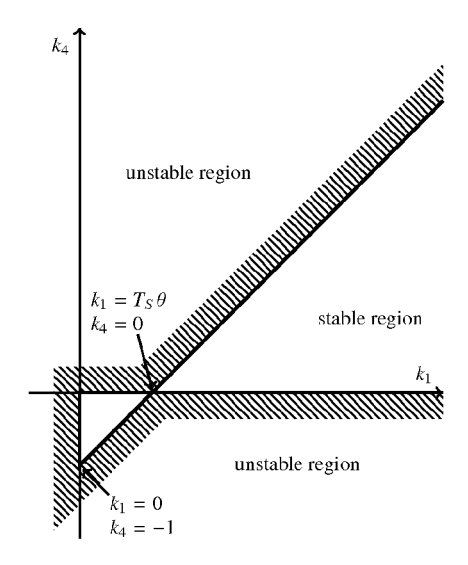


Fig. 11

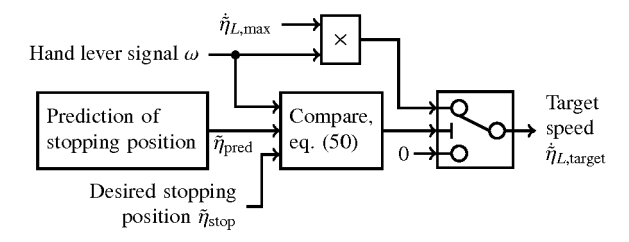
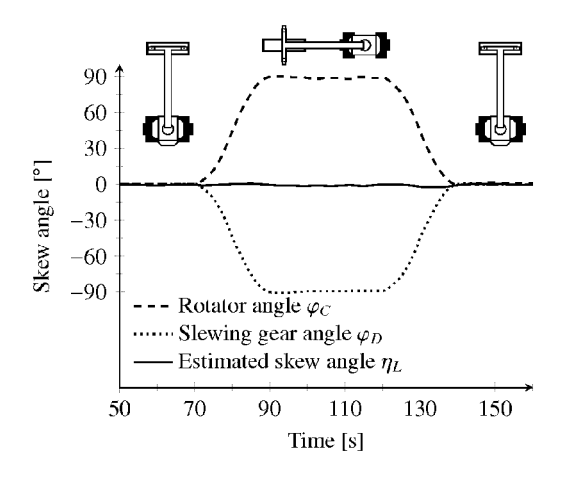


Fig. 12



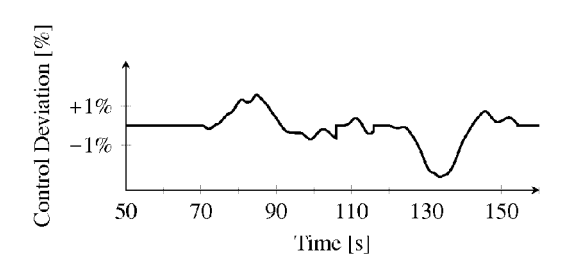
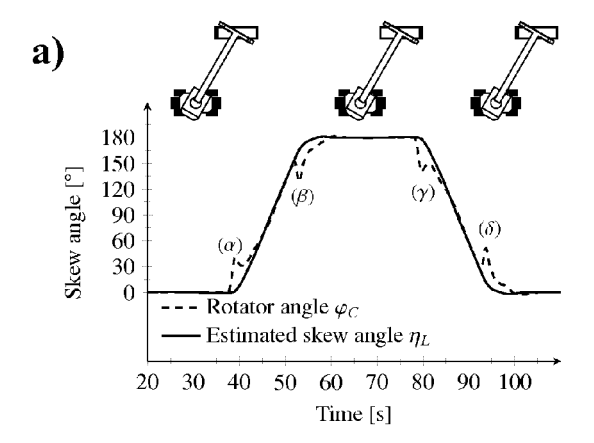
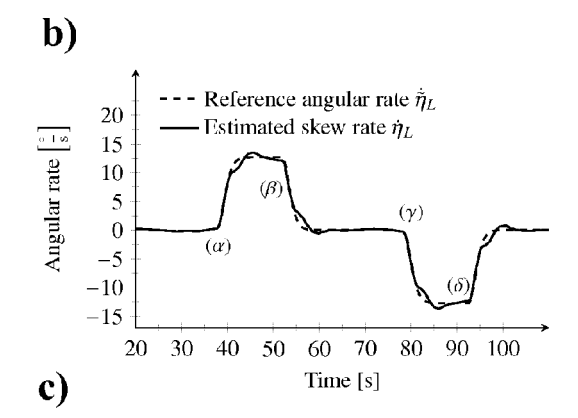
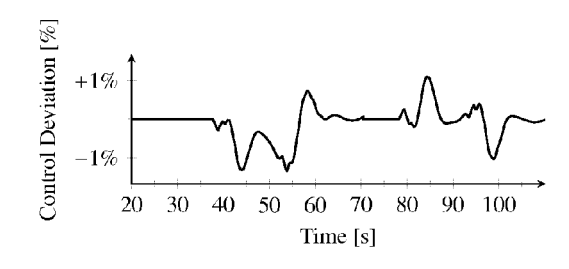


Fig. 13









EUROPEAN SEARCH REPORT

Application Number EP 15 16 9336

	Citation of document with in	ndication, where appropriate,	Relev	(ant	CLASSIFICATION OF THE
Category	of relevant passa		to cla		APPLICATION (IPC)
X Y	[AT]; SCHNEIDER KLA [DE];) 5 January 20 * paragraphs [0024]	IEBHERR WERK NENZING US [DE]; SAWODNY OLIVE 105 (2005-01-05) , [0031], [0033], [0060], [0062], [0064]	5-13	5 E	INV. B66C13/06 B66C13/08 B66C13/46
		, [0081], [0087] -			
Y	[AT]) 12 January 20	EBHERR WERK NENZING 11 (2011-01-12) , [0033] - [0037],	5-13		
A	DE 10 2006 048988 A NENZING [AT]) 24 Ap * abstract * * paragraphs [0056]	oril 2008 (2008-04-24)	1-15		
	* figures 1, 4, 11,				TECHNICAL FIELDS SEARCHED (IPC)
	The present search report has I	peen drawn up for all claims	1		
	Place of search	Date of completion of the search			Examiner
	The Hague	18 September 203	.5	Dijo	ux, Adrien
X : parti Y : parti	ATEGORY OF CITED DOCUMENTS cularly relevant if taken alone cularly relevant if combined with anotiment of the same category	T : theory or princip E : earlier patent do after the filing de	le underlyin cument, bu te in the applic	g the inve t publishe	ention

ANNEX TO THE EUROPEAN SEARCH REPORT ON EUROPEAN PATENT APPLICATION NO.

EP 15 16 9336

5

This annex lists the patent family members relating to the patent documents cited in the above-mentioned European search report. The members are as contained in the European Patent Office EDP file on The European Patent Office is in no way liable for these particulars which are merely given for the purpose of information.

Patent family

Publication

18-09-2015

Publication

15

Patent document

10

25

20

30

35

40

45

50

55

EP 1628902 A1 01-03-2 ES 2293271 T3 16-03-2 JP 4795228 B2 19-10-2 JP 2006525928 A 16-11-2 KR 20060021866 A 08-03-2 US 2006074517 A1 06-04-2 W0 2004106215 A1 09-12-2 EP 2272784 A1 12-01-2011 CN 101985343 A 16-03-2 DE 102009032267 A1 13-01-2 EP 2272784 A1 12-01-2 JP 2011016661 A 27-01-2 KR 20110004776 A 14-01-2 US 2011006025 A1 13-01-2 DE 102006048988 A1 24-04-2008 DE 102006048988 A1 24-04-2 EP 2033931 A1 11-03-2	EP 1628902 A1 01-03-20 ES 2293271 T3 16-03-20 JP 4795228 B2 19-10-20 JP 2006525928 A 16-11-20 KR 20060021866 A 08-03-20 US 2006074517 A1 06-04-20 W0 2004106215 A1 09-12-20 EP 2272784 A1 12-01-2011 CN 101985343 A 16-03-20 EP 2272784 A1 12-01-2011 EP 2272784 A1 12-01-20 EP 2272784 A1 12-01-20 IP 2011016661 A 27-01-20 KR 20110004776 A 14-01-20 US 2011006025 A1 13-01-20 US 2011006025 A1 13-01-20 EP 2033931 A1 11-03-20 ES 2534213 T3 20-04-20 JP 5396017 B2 22-01-20 JP 2008120596 A 29-05-20	EP 1628902 A1 01-03-2 ES 2293271 T3 16-03-2 JP 4795228 B2 19-10-2 JP 2006525928 A 16-11-2 KR 20060021866 A 08-03-2 US 2006074517 A1 06-04-2 W0 2004106215 A1 09-12-2 EP 2272784 A1 12-01-2011 CN 101985343 A 16-03-2 EP 2272784 A1 12-01-2 EP 2272784 A1 12-01-2 JP 2011016661 A 27-01-2 KR 20110004776 A 14-01-2 US 2011006025 A1 13-01-2 DE 102006048988 A1 24-04-2008 DE 102006048988 A1 24-04-2 EP 2033931 A1 11-03-2 ES 2534213 T3 20-04-2 JP 5396017 B2 22-01-2 JP 5396017 B2 22-01-2 JP 2008120596 A 29-05-2			date		member(s)		date
DE 102009032267 A1 13-01-2 EP 2272784 A1 12-01-2 JP 2011016661 A 27-01-2 KR 20110004776 A 14-01-2 US 2011006025 A1 13-01-2 DE 102006048988 A1 24-04-2008 DE 102006048988 A1 24-04-2 EP 2033931 A1 11-03-2	DE 102009032267 A1 13-01-20 EP 2272784 A1 12-01-20 JP 2011016661 A 27-01-20 KR 20110004776 A 14-01-20 US 2011006025 A1 13-01-20 DE 102006048988 A1 24-04-2008 DE 102006048988 A1 24-04-20 EP 2033931 A1 11-03-20 ES 2534213 T3 20-04-20 JP 5396017 B2 22-01-20 JP 2008120596 A 29-05-20	DE 102009032267 A1 13-01-2 EP 2272784 A1 12-01-2 JP 2011016661 A 27-01-2 KR 20110004776 A 14-01-2 US 2011006025 A1 13-01-2 DE 102006048988 A1 24-04-2008 DE 102006048988 A1 24-04-2 EP 2033931 A1 11-03-2 ES 2534213 T3 20-04-2 JP 5396017 B2 22-01-2 JP 2008120596 A 29-05-2	DE 10324692	A1	05-01-2005	EP ES JP JP KR US	1628902 2293271 4795228 2006525928 20060021866 2006074517	A1 T3 B2 A A A1	05-01-20 01-03-20 16-03-20 19-10-20 16-11-20 08-03-20 06-04-20
EP 2033931 A1 11-03-2	EP 2033931 A1 11-03-20 ES 2534213 T3 20-04-20 JP 5396017 B2 22-01-20 JP 2008120596 A 29-05-20	EP 2033931 A1 11-03-2 ES 2534213 T3 20-04-2 JP 5396017 B2 22-01-2 JP 2008120596 A 29-05-2	EP 2272784	A1	12-01-2011	DE EP JP KR	102009032267 2272784 2011016661 20110004776	A1 A1 A A	16-03-20 13-01-20 12-01-20 27-01-20 14-01-20 13-01-20
JP 5396017 B2 22-01-2 JP 2008120596 A 29-05-2			DE 102006048988	A1	24-04-2008	EP ES JP JP	2033931 2534213 5396017 2008120596	A1 T3 B2 A	24-04-20 11-03-20 20-04-20 22-01-20 29-05-20 03-07-20

REFERENCES CITED IN THE DESCRIPTION

This list of references cited by the applicant is for the reader's convenience only. It does not form part of the European patent document. Even though great care has been taken in compiling the references, errors or omissions cannot be excluded and the EPO disclaims all liability in this regard.

Patent documents cited in the description

- EP 1334945 A2 [0006]
- DE 10029579 [0007] [0028]

• DE 102006033277 A1 [0007] [0028]